THE JOURNAL OF BIOLOGICAL CHEMISTRY VOL. 286, NO. 11, pp. 9875–9887, March 18, 2011

Novel Androstenetriol Interacts with the Mitochondrial Translocator Protein and Controls Steroidogenesis*[S]

Received for publication, November 14, 2010, and in revised form, January 2, 2011 Published, JBC Papers in Press, January 5, 2011, DOI 10.1074/jbc.M110.203216

Andrew Midzak[‡§1], **Nagaraju Akula**[‡], **Laurent Lecanu**[‡§], **and Vassilios Papadopoulos**[‡§¶‖2]

From the [‡]*Research Institute of the McGill University Health Centre and the Departments of* [§]*Medicine,* [¶]*Biochemistry, and* [‖]*Pharmacology and Therapeutics, McGill University, Montreal, Quebec H3G 1A4, Canada*

Steroid hormones are metabolically derived from multiple enzymatic transformations of cholesterol. The controlling step in steroid hormone biogenesis is the delivery of cholesterol from intracellular stores to the cytochrome P450 enzyme CYP11A1 in the mitochondrial matrix. The 18-kDa translocator protein (TSPO) plays an integral part in this mitochondrial cholesterol transport. Consistent with its role in intracellular cholesterol movement, TSPO possesses a cholesterol recognition/interaction amino acid consensus (CRAC) motif that has been demonstrated to bind cholesterol. To further investigate the TSPO CRAC motif, we performed molecular modeling studies and identified a novel ligand, 3,17,19-androsten-5-triol (19-Atriol) that inhibits cholesterol binding at the CRAC motif. 19-Atriol could bind a synthetic CRAC peptide and rapidly inhibited hormonally induced steroidogenesis in MA-10 mouse Leydig tumor cells and constitutive steroidogenesis in R2C rat Leydig tumor cells at low micromolar concentrations. Inhibition at these concentrations was not due to toxicity or inhibition of the CYP11A1 enzyme and was reversed upon removal of the compound. In addition, 19-Atriol was an even more potent inhibitor of PK 11195-stimulated steroidogenesis, with activity in the high nanomolar range. This was accomplished without affecting PK 11195 binding or basal steroidogenesis. Finally, 19-Atriol inhibited mitochondrial import and processing of the steroidogenic acute regulatory protein without any effect on TSPO protein levels. In conclusion, we have identified a novel androstenetriol that can interact with the CRAC domain of TSPO, can control hormonal and constitutive steroidogenesis, and may prove to be a useful tool in the therapeutic control of diseases of excessive steroid formation.

Vertebrate steroid hormones are formed in response to stimulation of steroidogenic cells in the testes, ovaries, and adrenal cortex through the successive enzymatic transformation of cholesterol, the precursor of all steroids. Circulating pituitary peptide hormones, such as luteinizing hormone or chorionic gonadotropin in the gonads or adrenocorticotrophic hormone in the adrenal gland, bind to their cognate cell surface receptors, stimulating the synthesis of cAMP, the major second messenger of these hormone-receptor systems (1, 2). cAMP, in turn, promotes the traffic of cholesterol from cellular stores to the inner mitochondrial membrane, where it is metabolized to pregnenolone due to cholesterol side chain cleavage by the cytochrome P450 CYP11A1 (3). Pregnenolone undergoes further enzymatic transformation in the endoplasmic reticulum or mitochondria, giving rise to the final steroid products (4). The primary site of control in this process is the transport of cholesterol from intracellular sources across the double membrane of the mitochondria and into the matrix where CYP11A1 is located, a process that requires assistance of the cellular protein machinery that has recently been named the transduceosome (5, 6).

The transduceosome is assembled in response to hormone treatment and subsequent cAMP formation from both cytoplasmic and mitochondrial components to support and amplify the targeted response to the cAMP signal at the site where steroid formation begins. The cytosolic component that has attracted the greatest research attention is the steroidogenic acute regulatory protein (STAR)[3] (7, 8). STAR is rapidly synthesized in the cytoplasm in response to hormonal and cAMP stimulation as a 37-kDa protein containing a mitochondrial targeting sequence that is subsequently cleaved upon import into the mitochondria to generate a 30-kDa mature protein (9). Synthesis of STAR is stimulated by hormones and cAMP (10, 11), and *in vitro* overexpression studies have demonstrated that STAR elevates cholesterol trafficking into the mitochondria and steroid synthesis in steroidogenic cells (12). In addition, newly synthesized STAR has been shown to exert its action only at the outer mitochondrial membrane, and mature 30-kDa STAR in the mitochondrial matrix is inactive (13). At the outer mitochondrial membrane, STAR interacts with the mitochon-

* This work was supported, in whole or in part, by National Institutes of Health Grants ES007747 and HD037031. This work was also supported by Canadian Institutes of Health Research Grant MOP102647 and a Canada Research Chair in Biochemical Pharmacology (to V. P.). The Research Institute of the McGill University Health Centre was supported by a Center grant from Le Fonds de la Recherche en Santé du Québec. Drs. Akula, Lecanu, and Papadopoulos are named inventors in a patent pertaining to the work described here. The patent has been licensed to Samaritan Pharmaceuticals. Drs. Lecanu and Papadopoulos served in the past (until 2006) as consultants of Samaritan Pharmaceuticals.

[S] The on-line version of this article (available at http://www.jbc.org) contains supplemental Tables 1 and 2 and Figs. 1 and 2.

[1] Supported in part by Canadian Institutes of Health Research Postdoctoral Fellowship TGF36110.

[2] To whom correspondence should be addressed: The Research Institute of the McGill University Health Center, Montreal General Hospital, 1650 Cedar Ave., Montreal, Quebec H3G 1A4, Canada. Tel.: 514-934-1934 (ext. 44580); Fax: 514-934-8439; E-mail: vassilios.papadopoulos@mcgill.ca.

[3] The abbreviations used are: STAR, steroidogenic acute regulatory protein; START, STAR-related lipid transfer; 19-Atriol, 3,17,19-androsten-5-triol; CRAC, cholesterol recognition/interaction amino acid consensus; dbcAMP, dibutyryl-cAMP; DBI, diazepam binding inhibitor; hCG, human chorionic gonadotropin; 22*R*-HC, (22*R*)-hydroxycholesterol; PK 11195, 1-(2-chlorophenyl)-*N*-methyl-*N*-(1-methylpropyl)-3-isoquinolinecarboxamide; TSPO, translocator protein (18 kDa); Tricine, *N*-[2-hydroxy-1,1-bis(hydroxymethyl)-ethyl]glycine; RIA, radioimmunoassay; ANOVA, analysis of variance; TAT, transactivator of transcription.

drial voltage-dependent anion channel to exert its effects in a phosphorylation-dependent manner (14). STAR is phosphorylated by the cAMP-dependent protein kinase (15, 16). cAMP-dependent protein kinase also binds to PAP7 (peripheral-type benzodiazepine receptor- and cAMP-dependent protein kinase-associated protein 7)/ACBD3 (acyl-coenzyme A binding domain containing 3), a protein originally identified in a yeast two-hybrid screen (17) as a binding partner of the other integral mitochondrial membrane protein of the transduceosome, the peripheral-type benzodiazepine receptor, a protein later renamed TSPO (translocator protein 18 kDa) (18).

TSPO was first identified in the 1970s by observation of radiolabeled benzodiazepine receptor sites in the kidney (19). These sites were subsequently found to consist of voltage-dependent anion channel and TSPO complexes (20). TSPO, which is highly expressed in steroidogenic tissues (18), has been extensively characterized pharmacologically and observed to bind various small molecules (21). The most prominent of these small molecules has been the isoquinoline carboxamide PK 11195, which binds to TSPO with high affinity (22). In addition to synthetic ligands, TSPO binds endogenous compounds, including the polypeptide diazepam binding inhibitor (DBI/ACBD1) (23) and porphyrins (24). However, the endogenous TSPO ligand of greatest interest for steroidogenesis is cholesterol (25, 26), the metabolic precursor for steroid biosynthesis. TSPO binds cholesterol with high affinity through a cholesterol recognition/interaction amino acid consensus (CRAC) motif at its carboxyl terminus (27, 28).

The CRAC motif ((L/V)X_{1-5}YX_{1-5}(R/K)) has been characterized in several proteins that interact with cholesterol (29–31). Hydropathy profile and experimental analysis have suggested that TSPO possesses a five-transmembrane structure (32, 33), findings recently supported by electron cryomicroscopy of a bacterial homolog (34). Deletion of the C terminus of recombinant mammalian TSPO, which contains the CRAC motif, severely reduced cholesterol uptake when expressed in *Escherichia coli*, although PK 11195 binding was retained (25). These findings suggested distinct drug ligand and cholesterol binding sites in TSPO. Much of our understanding of the involvement of TSPO in steroidogenesis, however, has been derived from work with drug ligands. TSPO ligands, such as PK 11195, stimulate steroidogenesis and cholesterol flux in various systems (35, 36). A peptide agonist identified to displace drug ligand binding to TSPO inhibited hormone-mediated steroidogenesis in a Leydig cell tumor cell model (37), further confirming the importance of the drug binding site. However, effective tools to study the CRAC domain of TSPO *in vitro* and *in vivo* are lacking. Transduction of a TSPO CRAC peptide attached to the HIV-1 TAT peptide for transduction efficiency was found to inhibit steroidogenesis, presumably through competition with the CRAC domain (27). Similar to work performed with TSPO drug domain ligands, a ligand for the CRAC domain of TSPO would be a highly effective tool to study transduceosome function and cholesterol movement.

Here, we report the identification of a novel ligand for the CRAC domain of TSPO. Computational modeling of the CRAC domain and *in silico* screening yielded a spectrum of compounds belonging to several chemical families. Bioactivity screening yielded a novel androstenetriol, 3,17,19-androsten-5-triol (19-Atriol), that was found to compete with promegestone cross-linking to a CRAC peptide but left PK 11195 binding unaffected. Kinetic analysis of steroidogenic inhibition revealed rapid suppression of steroid biosynthesis in response to hormonal and drug-mediated stimulation. Protein analysis of transduceosome components revealed that 19-Atriol suppressed STAR mitochondrial import, supporting a gating mechanism for TSPO in steroidogenesis. These findings provide the first evidence for a novel ligand for the CRAC domain of TSPO and underscore the central role for TSPO in steroidogenesis.

EXPERIMENTAL PROCEDURES

Materials—[1,2,6,7-^{3}H]Progesterone (specific activity, 101.3 Ci/mmol), [17α-*methyl*-^{3}H]promegestone (specific activity, 84.6 Ci/mmol), and [^{3}H]PK 11195 (1-(2-chlorophenyl)-*N*-methyl-*N*-(1-methyl-propyl)-3-isoquinoline carboxamide) (specific activity, 89.8 Ci/mmol) were obtained from PerkinElmer Life Sciences. Progesterone was obtained from Sigma-Aldrich. Cell culture supplies were purchased from Invitrogen. Tissue culture plasticware was purchased from Corning Glass. Electrophoresis reagents and materials were supplied from NOVEX of Invitrogen. Small molecule inhibitors for biological screening were obtained from Chembridge (San Diego, CA), InterBioscreen (Moscow, Russia), and the University of Florida Department of Chemistry. All other chemicals used were of analytical grade and were obtained from various commercial sources.

Cell Culture—MA-10 mouse Leydig tumor cells were a gift from Dr. Mario Ascoli (University of Iowa). Cells were cultured in 75-cm^2 cell culture flasks with Dulbecco's modified Eagle's medium (DMEM)/nutrient mixture F-12 Ham supplemented with 5% fetal bovine serum and 2.5% heat-inactivated horse serum, as described previously (38). R2C cells were from ATCC (Manassas, VA), derived from rat Leydig tumors (39), and cultured under conditions similar to those for MA-10 cells.

Computational Modeling—Modeler6v2 (40) was used to build the homology models. The input alignment for the Modeler was obtained with BlastP (41) searches based on the sequences of mouse, rat, and human CRAC peptides from TSPO. Subsequently, these models were built from the crystal structures of Protein Data Bank entries 1A99 (42) and 1P9M (43). The cholesterol molecular structure was docked into the active site, and the complex energy was minimized using ESFF of the Insight 2000 program. The Unity4.3 module from Tripos (St. Louis, MO) was used for the pharmacophore and similarity searches (44), and molecular docking programs such as FlexiDock (Tripos) and FlexX (45) were used to filter the structures for virtual screening. The ligand and protein complexes were energy-minimized with 5000 iterations of the conjugate gradient algorithm such that the square root of the average magnitude of the force was less than or equal to 0.01 kcal/(mol·Å). Glide 4.5 (Schrodinger, Portland, OR) and Gold 4.1 (Cambridge Crystallographic Data Centre, Cambridge, CA) programs were used to evaluate the docking scores and to design new structures. The physicochemical properties of the various ligands tested (log *P*, log *D*, and number of hydrogen bond donors and acceptors) were calculated using the software Marvin (ChemAxon Ltd., Budapest, Hungary).

[^{3}H]Promegestone Photolabeling—[^{3}H]Promegestone photolabeling of synthetic CRAC peptides was performed as described previously (27). Briefly, 150 μM synthetic TAT-CRAC peptide in phosphate-buffered saline (PBS) was incubated with [^{3}H]promegestone at a final concentration of 120 nM in the absence or presence of 0–100 μM cholesterol or 19-Atriol in a 100-μl final volume. After a 1-h incubation at 4 °C, samples were photoirradiated for 30 min at a distance of 0.5 cm using UV light with a maximum emission at 366 nm (Ultraviolet Products, Gabriel, CA). Sample loading buffer was applied to the samples, and then they were subjected to SDS-PAGE using the Tricine buffer system from NOVEX. Proteins were then transferred to a nitrocellulose membrane. The membrane was either exposed to a tritium-sensitive screen and analyzed using a Cyclone Storage phosphor system (Packard) or exposed to tritium-sensitive film (Fujifilm). Image analysis of the phosphor images was performed using OPTIQUANT software from Packard for the tritium-sensitive screen or Multi Gauge software from Fujifilm for tritium-sensitive film.

[^{3}H]PK 11195 Radioligand Binding Assays—[^{3}H]PK 11195 binding to 10 μg of MA-10 cell homogenate was performed as described previously (45). Specific [^{3}H]PK 11195 binding was analyzed using the iterative nonlinear curve-fitting program in Prism 4 from GraphPad (La Jolla, CA).

Steroid Biosynthesis—For steroid synthesis experiments in the presence of medium with human chorionic gonadotropin (hCG), dibutyryl-cAMP (dbcAMP), (22*R*)-hydroxycholesterol (22*R*-HC), or PK 11195, MA-10 cells were plated into 96-well plates at 5×10^4 cells/well. After allowing cells to adhere for 3–18 h, the cells were washed with PBS and exposed to the respective treatment (medium alone or 50 ng/ml hCG, 1 mM dbcAMP, 20 μM 22*R*-HC, or 1 μM PK 11195 in medium) in the presence or absence of the prospective CRAC ligand under investigation. All medium conditions were serum-free. The hCG and dbcAMP stocks were prepared in cell culture medium or water. The 22*R*-HC, PK 11195, and CRAC ligand stocks were prepared as ethanolic stock solutions and used at a final ethanol concentration of $<$0.02% in media. Controls contained the same amount of ethanol. For the two-phase analysis of 19-Atriol inhibition of steroidogenesis, cells were preincubated with either medium or 19-Atriol. In phase two, the cells were incubated with either 50 ng/ml hCG or 50 ng/ml hCG plus 0–100 μM 19-Atriol for 1 h or with medium for 1 h and 50 ng/ml hCG for an additional 1 h. At the end of the incubation, culture medium was collected and tested for progesterone production using radioimmunoassay (RIA) with progesterone antisera (MP Biomedicals, Solon, OH), following the manufacturer's recommended conditions. Progesterone production was normalized for the amount of protein in each well. RIA data were analyzed using Prism 4.02 from GraphPad.

Mitochondrial Integrity/Cell Viability—Cell viability and mitochondrial integrity at the end of the incubation protocols described above were assessed using the 3-(4,5-dimethylthiazol-2-yl)-2,5-diphenyltetrazolium bromide cell proliferation kit for mitochondrial integrity (46) (Roche Applied Science). Formazan blue formation was quantified at 600 and 690 nm using the Victor quantitative detection spectrophotometer (PerkinElmer Life Sciences), and the results were expressed as ($OD_{600} - OD_{690}$).

Protein Measurement—Proteins were quantified using the dye-binding assay of Bradford (47) with bovine serum albumin (BSA) as the standard.

Immunoblot (Western Blot) Analysis—After treatment, MA-10 cells were washed with PBS and then sample buffer (25 mM Tris-HCl, pH 6.8, 1% SDS, 5% β-mercaptoethanol, 1 mM EDTA, 4% glycerol, and 0.01% bromphenol blue) was added. Proteins were separated by electrophoresis onto a 4–20% SDS-PAGE gradient gel and electrophoretically transferred to a nitrocellulose membrane as described previously (27). Membranes were incubated with primary antibodies against TSPO (1:2,500) (27), STAR (48) (1:5,000) (48), and GAPDH (1:10,000) (Trevigen, Gaithersburg, MD). The 18-kDa TSPO and 30-kDa STAR proteins were visualized using an ECL kit (Amersham Biosciences) and HRP-goat anti-rabbit and HRP-rabbit anti-mouse secondary antisera used at 1:7,000 and 1:5,000 dilutions, respectively. Densitometric image analysis of the immunoreactive protein bands was performed using Multi Gauge software.

Statistical Analysis—Statistical analysis was performed using Student's *t* test and one-way ANOVA followed by the Student Newman-Keuls test, using the Prism 4.02 software package from GraphPad.

RESULTS

Computational Modeling of the TSPO CRAC Domain—We undertook a structure-based approach to design specific inhibitors for TSPO by using homology modeling, which has been successfully used to generate new ligands against several different classes of drug targets. A comparison of the sequence alignment of vertebrate TSPO CRAC domains from mice, rats, and humans revealed a high degree of sequence identity (Fig. 1*A*). Input alignments for computational modeling with Modeler were obtained with BlastP (41), and the homology models were built from the crystal structures of the putrescine (42) and interleukin-6 receptors (43). Cholesterol, the endogenous ligand for this motif, was docked into the active site, and the ligand-protein complex was optimized (Fig. 1*B*).

In most cases, methods for structure-based lead generation are based on computational descriptions of a binding site. Commonly used descriptors for such binding sites are the spatial coordinates of atoms or pharmacophores. For the current study, we used human and mouse homology models of the TSPO CRAC motif for the identification of novel CRAC ligands. The cholesterol binding site of TSPO formed a deep cleft between Tyr^{152} and Arg^{158}, with cholesterol filling this cleft (Fig. 1*B*). The two most important hydrogen bond donors, Tyr^{152} and Arg^{158}, were subsequently used for the pharmacophore search. In addition, the hinge region of the motif close to Cys^{153} was used as a hydrophobic pharmacophore, as were Thr^{148} and Leu^{150}. Finally, the region around Asn^{151} served as a hydrophilic pharmacophore (Fig. 1, *A* and *C*). The acceptor and donor sites of the Flex pharmacophores were defined without distance constraints, and by using a receptor site module, exclusion spheres were modeled up to a 5-Å region from the pharmacophore site. To obtain highly selective and potent TSPO inhibitors at the CRAC region, we used the above defined phar-

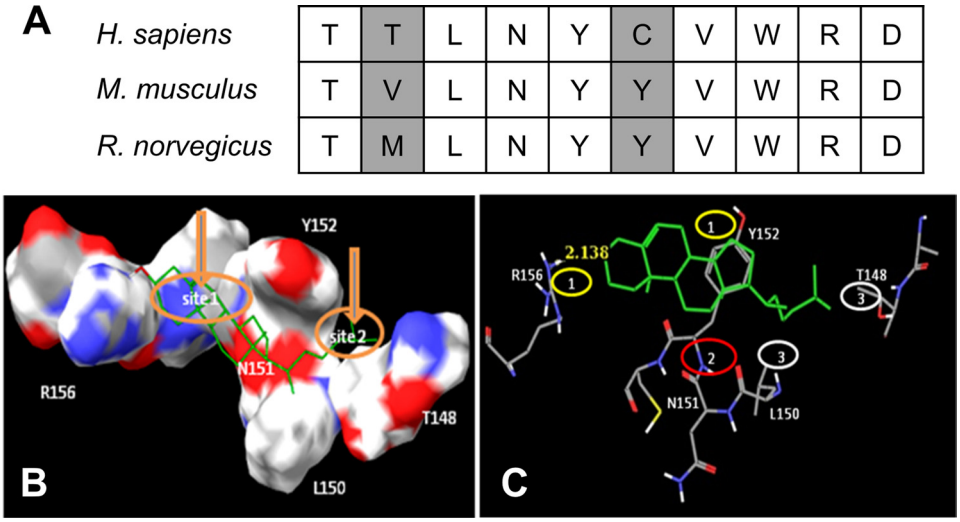

FIGURE 1. **Computational modeling of the TSPO CRAC domain.** *A*, sequence alignment of mammalian TSPO CRAC domains used for *in silico* modeling. *B*, computational molecular surface model of human TSPO CRAC domain fit with cholesterol. Active site residues are mapped with their chemical properties (*red*, negatively charged; *blue*, positively charged). Molecular binding pockets are denoted as site 1 and site 2. *C*, defined pharmacophore atoms of CRAC domain docked with cholesterol. *Yellow circles* (*1*), hydrogen bond donors; *red circles* (*2*), hydrophilic sites; *gray circles* (*3*), hydrophobic pharmacophores.

macophores and virtually screened the commercially available steroid and non-steroidal databases using two-dimensional Unity searches and identified ~700 steroid-substituted and non-steroidal small molecule structures targeted against the cholesterol binding site of TSPO.

These compounds were docked to the cholesterol binding site using several molecular docking programs (45, 49, 50) to rank-order the compounds using a consensus scoring function, CScore (a combination of various docking scores like G_Score, D_Score, ChemScore, and PMF_score) (51). The 70 highest scoring structures were selected and manually viewed for their three-dimensional graphical orientation, mode of binding, and diversity. Structures that docked with proper orientation and with intermolecular hydrogen bonding were selected for a further round of minimization. The highest scoring compounds of this screening round and their protein complexes were further energy-minimized using an extensible systematic force field to better fit the ligands into the cholesterol binding pocket. The binding orientation of cholesterol is shown in Fig. 1*C*, and additional identified structural models are presented in supplemental Table 1. Based on the above factors, the best 19 structures were selected for testing in a biological assay.

Chemical Clustering and Bioactivity of CRAC Ligands—Pharmacophore screening provided a set of compounds predicted to bind the CRAC domain based on their docking scores, measure of steric fit, and their chemical binding energy (supplemental Table 2). Graphing these compounds according to their respective scores demonstrated a linear correlation (Pearson $r = 0.72$) (Fig. 2*A*). Interestingly, compounds ranked in this manner appeared to cluster based on their structures, with those containing aromatic chemical backbones clustering with higher predicted binding scores (Fig. 2, *gray triangles*) and those with steroid backbones clustering with comparatively lower predicted binding scores (Fig. 2, *black circles*). To ascertain the similarity and differences between the compounds, we hierarchically clustered the compounds using the online NCBI PubChem clustering toolkit (available from the NCBI site). This revealed three families of compounds proposed to interact with the CRAC domain, based on qualitative observations: (i) benzoic acids and amides, (ii) substituted steroids, and (iii) substituted steroids containing a large aliphatic group (Fig. 2*B*).

Previous studies with transduced TAT-CRAC peptide inhibited hormone-stimulated steroidogenesis in MA-10 mouse Leydig tumor cells, implicating the CRAC domain in mitochondrial cholesterol transport during steroidogenesis (27). These findings also suggest that a ligand binding the CRAC domain will similarly inhibit steroid production in this model system. To explore this hypothesis, we conducted a bioactivity screen of our hypothesized CRAC ligands using MA-10 Leydig cells exposed to 1 mM dbcAMP coincubated with a 10 μM concentration of the selected CRAC ligands. As shown in Fig. 3*A*, three of the 19 compounds could significantly inhibit progesterone production stimulated by dbcAMP for 2 h, with the most potent, 5936472 (3,17,19-androsten-5-triol, referred to hereafter as 19-Atriol), inhibiting steroidogenesis by nearly 75%. The steroid adducts 7384616 and 59572117 also significantly inhibited steroidogenesis but to a lesser degree. The ability of the compounds to inhibit steroidogenesis was not a function of their solubility because plotting percentage inhibition *versus* log *D* values revealed no correlation (Fig. 3*B*; Pearson $r = 0.002$ and 0.051 at pH 7.0 and 7.4, respectively). Molecular docking of 19-Atriol is shown in Fig. 3*C*.

Effect of CRAC Ligands on TSPO Binding Parameters—The above modeling studies described potential CRAC ligands, and our bioactivity assays supported this hypothesis for several of these compounds. To affirm the interaction of CRAC ligands with the TSPO CRAC domain, we employed a previously utilized [^{3}H]promegestone binding assay using synthetic TAT-CRAC peptides that qualitatively demonstrate the molecular interaction of the putative ligands with the CRAC motif (27). As seen in Fig. 4, *A* and *C*, cholesterol dose-dependently inhibited [^{3}H]promegestone cross-linking to the 3.2-kDa TAT-CRAC peptide between 0 and 100 μM with maximal inhibition at 100 μM, consistent with previous reports (27). 19-Atriol also dose-

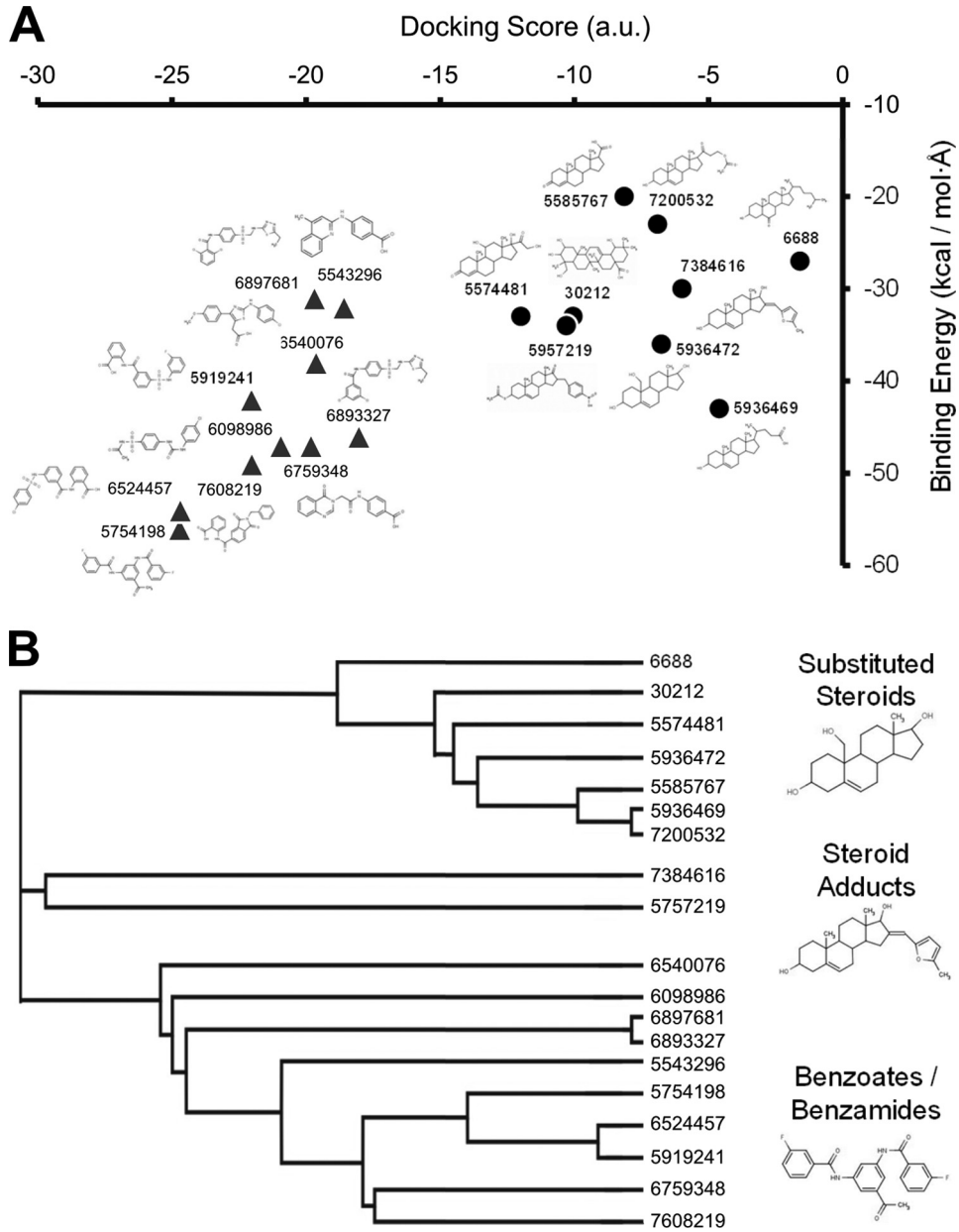

FIGURE 2. ***In silico* scoring of CRAC ligands and hierarchical clustering into molecular species.** *A*, computational CRAC ligand scoring and ranking of docking scores (in arbitrary units (*a.u.*)) *versus* binding energy (in kcal-mol·Å). Ranking revealed the compounds to cluster into two groups: benzoate/benzamide backbones (*black circles*) and steroid backbones (*gray circles*). Compound ID number and structure are shown *beside* scores. *B*, hierarchical chemical clustering of CRAC ligands. Clustering of the CRAC ligands delineated three chemically distinct groups: substituted steroids (*top*), steroid adducts (*middle*), and benzoates/benzamides (*bottom*). Compound ID number is listed *beside* the tree leaf and example structures shown *below* the group title. Chemical names and structures of all compounds are included in supplemental Table 1.

dependently inhibited [^{3}H]promegestone cross-linking to the 3.2-kDa TAT-CRAC peptide between 0 and 100 μM (Fig. 4, *B* and *C*). Although 19-Atriol inhibited [^{3}H]promegestone cross-linking, like cholesterol, it was not as effective at eliciting maximal displacement (Fig. 4*C*). Comparison of the IC_{50} for displacement of [^{3}H]promegestone further supported that cholesterol (IC_{50} = 1.1 μM) is a better ligand for the CRAC motif than 19-Atriol (IC_{50} = 23.2 μM). These results demonstrate that 19-Atriol is a *bona fide* TSPO CRAC ligand.

TSPO can bind both drug ligands, such as the isoquinoline carboxamide PK 11195, and cholesterol (22), and deletion mutation analyses of TSPO have indicated that deletion of the C terminus containing the CRAC domain may impair drug ligand binding (25). To examine the relationship between 19-Atriol interaction with TSPO and PK 11195 binding, MA-10 mitochondrial preparations were incubated with 19-Atriol, and the specific binding of [^{3}H]PK 11195 was measured. As shown in the saturation isotherm in Fig. 4*D*, 19-Atriol did not affect PK 11195 specific binding to MA-10 mitochondria, with the principal binding site observed in these assays being TSPO (36). Further analysis of the data also revealed no significant changes to the B_{max} and K_D of PK 11195 binding to these samples (Fig. 4, *E* and *F*). Thus, 19-Atriol does not affect the PK 11195 drug binding site of TSPO.

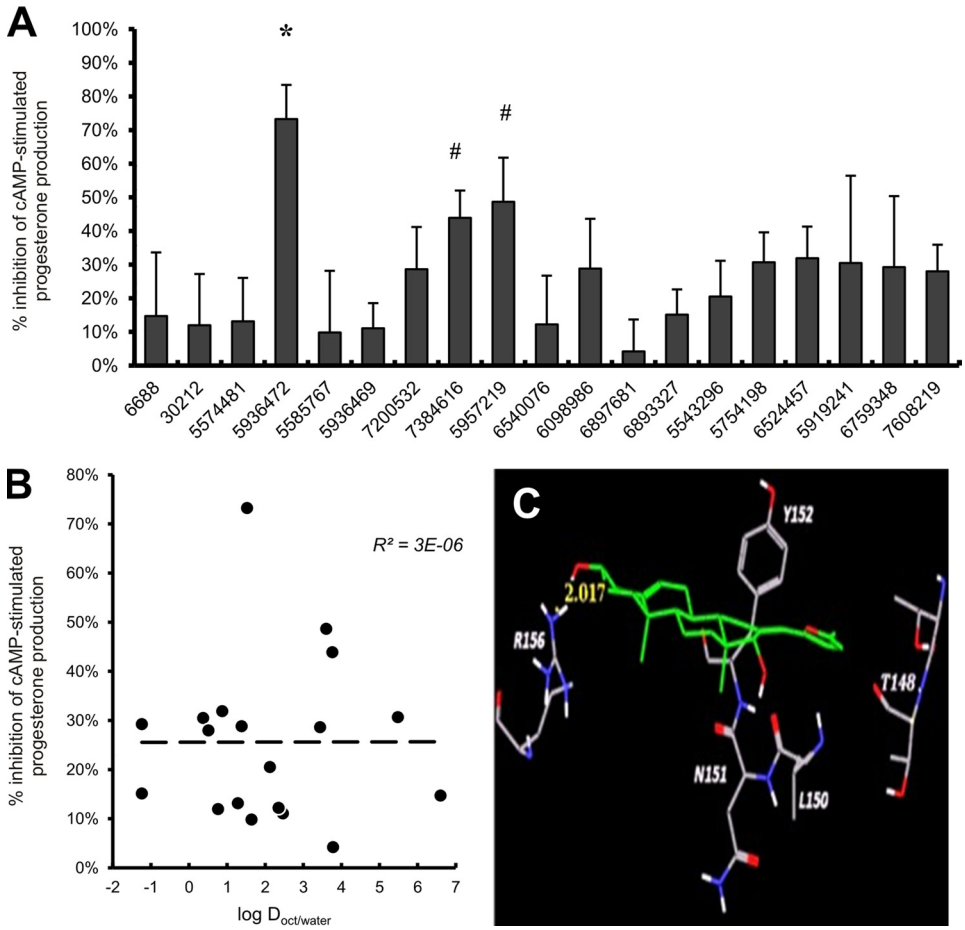

FIGURE 3. **Screening of CRAC ligands bioactivity.** *A*, effect of substituted steroid, steroid adduct, and benzoate/benzamide CRAC ligands on cAMP-stimulated progesterone production by MA-10 mouse tumor Leydig cells. Cultures were incubated with 1 mM dbcAMP plus 10 μM of the respective CRAC ligand for 2 h. Progesterone levels in the medium were assessed by RIA. Data are presented as the mean percentage inhibition of control progesterone production ± S.E. (*error bars*). *, $p < 0.001$; #, $p < 0.05$ by one-way ANOVA with Newman-Keuls test. *B*, relationship between percentage inhibition of cAMP-stimulated steroidogenesis and solubility of the CRAC ligands in aqueous medium, denoted by log *D*, the logarithm of the solubility distribution coefficient between octanol and water. *C*, CRAC ligand 5936472 (19-Atriol) docking conformation. 19-Atriol is shown in *green*.

Toxicity of the CRAC Ligand 19-Atriol—Binding assays with [^{3}H]promegestone and [^{3}H]PK 11195 demonstrated binding of 19-Atriol to the CRAC domain of TSPO and showed that this binding did not perturb PK 11195 binding to TSPO. Questions still remain as to the specificity of the bioactivity of 19-Atriol in suppressing steroid biosynthesis. TSPO has been implicated in the mitochondrial permeability transition and cell death (52), and 19-Atriol could be facilitating cell death through CRAC domain binding, thus inhibiting steroidogenesis. To investigate this hypothesis, we cultured MA-10 cells for 24 h with increasing concentrations of 19-Atriol and examined these cultures for evidence of cell death. As shown in Fig. 5*A*, 19-Atriol up to 10 μM had no effect on cellular morphology or protein content (data not shown). To further examine the cellular toxicity of 19-Atriol, we assessed viability and mitochondrial integrity using the 3-(4,5-dimethylthiazol-2-yl)-2,5-diphenyltetrazolium bromide assay based on the reduction of mitochondrial diaphorase. As shown in Fig. 5*B*, a range of 19-Atriol concentrations in medium for 2 h exhibited no detectable toxicity. MA-10 cells can be metabolically activated by hormonal stimulation (53), and such metabolic stimulation might expose latent toxicity unobservable without hormonal stimulation; thus, we performed similar experiments with the addition of 50 ng/ml hCG. As shown in Fig. 5*C*, 19-Atriol did not exhibit any effect on viability or mitochondrial integrity upon metabolic stimulation, demonstrating that inhibition of steroidogenesis by this compound was due to its binding to the CRAC domain and not an inherent toxicity.

Characterization of Steroidogenic Inhibition by 19-Atriol—Our single-point bioactivity screen had demonstrated the ability of 19-Atriol to control steroidogenesis. The dose-response effect of 19-Atriol on steroidogenesis was further characterized by stimulating MA-10 cells with 50 ng/ml hCG in the presence of increasing concentrations of 19-Atriol for 2 h (Fig. 6*A*). Significant inhibition of progesterone synthesis was observed beginning at 1 μM 19-Atriol, with an IC_{50} of 3.58 ± 1.56 μM. This inhibition of progesterone production by 19-Atriol correlated linearly with its ability to displace [^{3}H]promegestone from the TAT-CRAC peptide (Fig. 6*A*, *inset*, $R^2 = 0.98$). Progesterone, however, is not a direct marker of cholesterol transfer but rather the product of 3β-HSD metabolism of pregnenolone, which is the product of CYP11A1 metabolism of cholesterol. Moreover, CYP11A1 possesses a CRAC domain in its active site (25, 54) that 19-Atriol may be inhibiting. To affirm that 19-Atriol is inhibiting cholesterol flux and not CYP11A1 met-

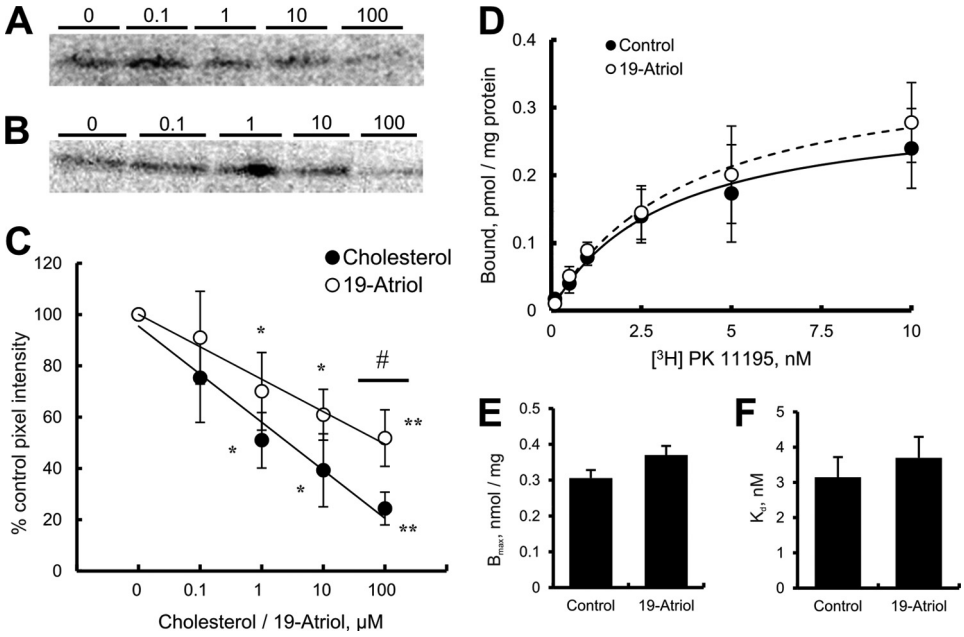

FIGURE 4. **Effect of 19-Atriol on TSPO binding parameters.** *A* and *B*, binding and cross-linking of [^{3}H]promegestone to synthetic TAT-CRAC peptide in the presence of increasing concentrations (0.1–100 μM) of cholesterol (*A*) and 19-Atriol (*B*). A representative autoradiograph of three independent experiments is shown. *C*, quantification of [^{3}H]promegestone cross-linking to synthetic TAT-CRAC peptide in the presence of increasing concentrations (0.1–100 μM) of cholesterol and 19-Atriol. The mean ± S.E. (*error bars*) of three independent experiments is presented. *, $p < 0.05$; **, $p < 0.01$ by one-way ANOVA. *D*, saturation isotherm of [^{3}H]PK 11195 binding to isolated MA-10 mitochondria in the presence and absence of 10 μM 19-Atriol. The mean ± S.E. of three independent mitochondrial preparations and binding experiments is shown. *E* and *F*, effect of 19-Atriol on B_{max} (*E*) and K_d (*F*) of PK 11195 binding to MA-10 mitochondria (from *D*). Results shown are the mean ± S.E. of three independent mitochondrial preparations and binding experiments.

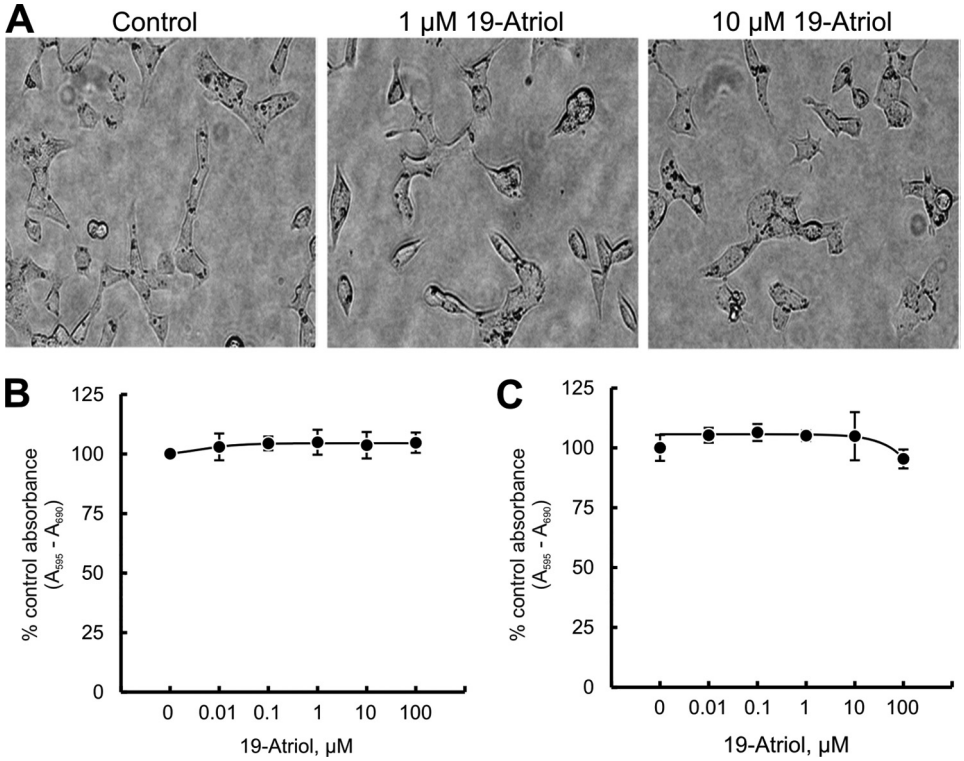

FIGURE 5. **19-Atriol and cellular and mitochondrial toxicity.** *A*, effect of 19-Atriol on cellular morphology after extended exposure. MA-10 cultures were exposed to 19-Atriol (0–10 μM) in medium for 24 h, and then cellular morphology was imaged via light microscopy at ×10 magnification. Representative images from three independent experiments are shown. *B* and *C*, cell viability and mitochondrial integrity were determined using the 3-(4,5-dimethylthiazol-2-yl)-2,5-diphenyltetrazolium bromide assay after incubating cell cultures with increasing concentrations of 19-Atriol (0–10 μM) in the presence of medium (*B*) or 50 ng/ml hCG (*C*). Results are expressed as the mean ± S.E. (*error bars*) percentage control assay absorbance from three independent experiments.

abolic activity, experiments were performed with 22*R*-HC, a soluble cholesterol analog that bypasses mitochondrial cholesterol transport, in the presence of increasing concentrations of 19-Atriol. As shown in Fig. 6*B*, a concentration of 100 μM 19-Atriol inhibited the CYP11A1-mediated metabolism of cholesterol. However, 19-Atriol did not demonstrate a significant

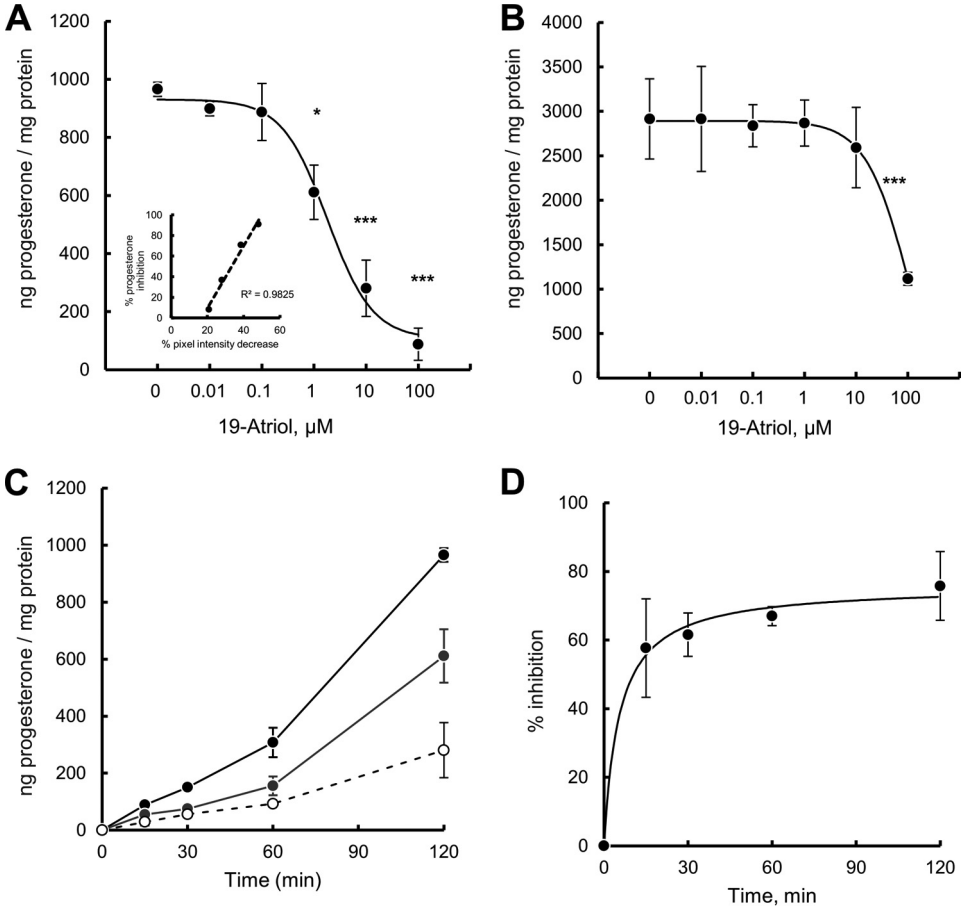

FIGURE 6. **19-Atriol and hormonally stimulated steroid biosynthesis.** *A*, dose-dependent effects of 19-Atriol on hormone-driven steroidogenesis. MA-10 cells were cultured with increasing concentrations of 19-Atriol (0–100 μM) for 2 h in the presence of 50 ng/ml hCG, and then progesterone production was assessed by RIA. Results are presented as the mean ± S.E. (*error bars*). ***, $p < 0.001$; *, $p < 0.05$ by one-way ANOVA with Neumann-Keuls test. *Inset*, correlation between percentage of TAT-CRAC promegestone displacement by 19-Atriol shown in Fig. 4*C* compared with percentage of hCG-stimulated progesterone production shown in *A*. *B*, 19-Atriol and 22*R*-HC-dependent steroidogenesis. Cell cultures were incubated with 20 μM 22*R*-HC and increasing concentrations of 19-Atriol (0–10 μM) for 2 h, and steroid production was assessed by RIA. Results are presented as the mean ± S.E. ***, $p < 0.001$ by one-way ANOVA with Neumann-Keuls test. *C*, time-dependent effects of 19-Atriol on hormone-dependent steroidogenesis. MA-10 cells were cultured with 0 (*black circles* and *line*), 1 (*gray circles* and *line*) or 10 μM (*open circles* and *dashed line*) 19-Atriol in the presence of 50 ng/ml hCG for 0–120 min, and progesterone synthesized was assessed at 15, 30, 60, and 120 min. Mean ± S.E. values are shown for each time point. All 19-Atriol incubations were significantly different from control cultures ($p < 0.05$ by one-way ANOVA); the 120-min incubations with 1 and 10 μM 19-Atriol were significantly different from each other as well ($p < 0.05$). *D*, hyperbolic plot of steroidogenic inhibition by 10 μM 19-Atriol, demonstrating rapid and nearly maximal inhibition of steroidogenesis by 19-Atriol within 15 min.

effect in the concentration range that inhibits hormone-stimulated steroidogenesis (1–10 μM).

Steroid biosynthesis occurs very rapidly in response to hormonal stimulation (36), and examination of the kinetics of TSPO-mediated steroidogenesis has shown that it is necessary for the initiation of steroidogenesis (38). To determine whether 19-Atriol can similarly inhibit steroidogenesis in such a rapid manner, MA-10 cell cultures were stimulated with 50 ng/ml hCG in the presence of 10 μM 19-Atriol, and then progesterone production was measured in the medium between 0 and 120 min. As shown in Fig. 6*C*, 19-Atriol significantly inhibited progesterone production throughout the 120-min time course. Replotting the data as percentage inhibition revealed that the 19-Atriol-induced steroidogenic inhibition observed with 10 μM 19-Atriol reached 60–70% within 15 min and did not increase with further exposure (Fig. 6*D*). These results demonstrate that binding of 19-Atriol caps the amount of cholesterol transferred into the mitochondria in a dose- and time-dependent manner.

The calculated log *D* of 19-Atriol (1.52 at pH 7.0 and 7.2) suggested that this compound was readily water-soluble (Fig. 3*B*). This prediction was consistent with the rapid ability of 19-Atriol to inhibit steroidogenesis, suggesting ready association with the CRAC domain of TSPO at the outer mitochondrial membrane (Fig. 6, *C* and *D*). It was thus of interest to examine whether 19-Atriol remained associated with the cells following its removal from the medium. In the absence of a radiolabeled form of 19-Atriol, we developed a two-phase assay to address this question (Fig. 7*A*). In the first phase, MA-10 cells were treated with either 0–100 μM 19-Atriol or medium for 1 h. The cells were then washed briefly with PBS and then stimulated in a second phase for 1 h with 50 ng/ml hCG plus 0–100 μM 19-Atriol or 50 ng/ml hCG for 1 h. In parallel experiments, cells were cultured in medium for 1 h following a 1-h exposure to 0–100 μM 19-Atriol to ensure extended wash-out, followed by stimulation with 50 ng/ml hCG for 1 h. Consistent with the hypothesis that 19-Atriol acts immediately, pre-exposure of cells to 19-Atriol had no further appreciable effect on cells incu-

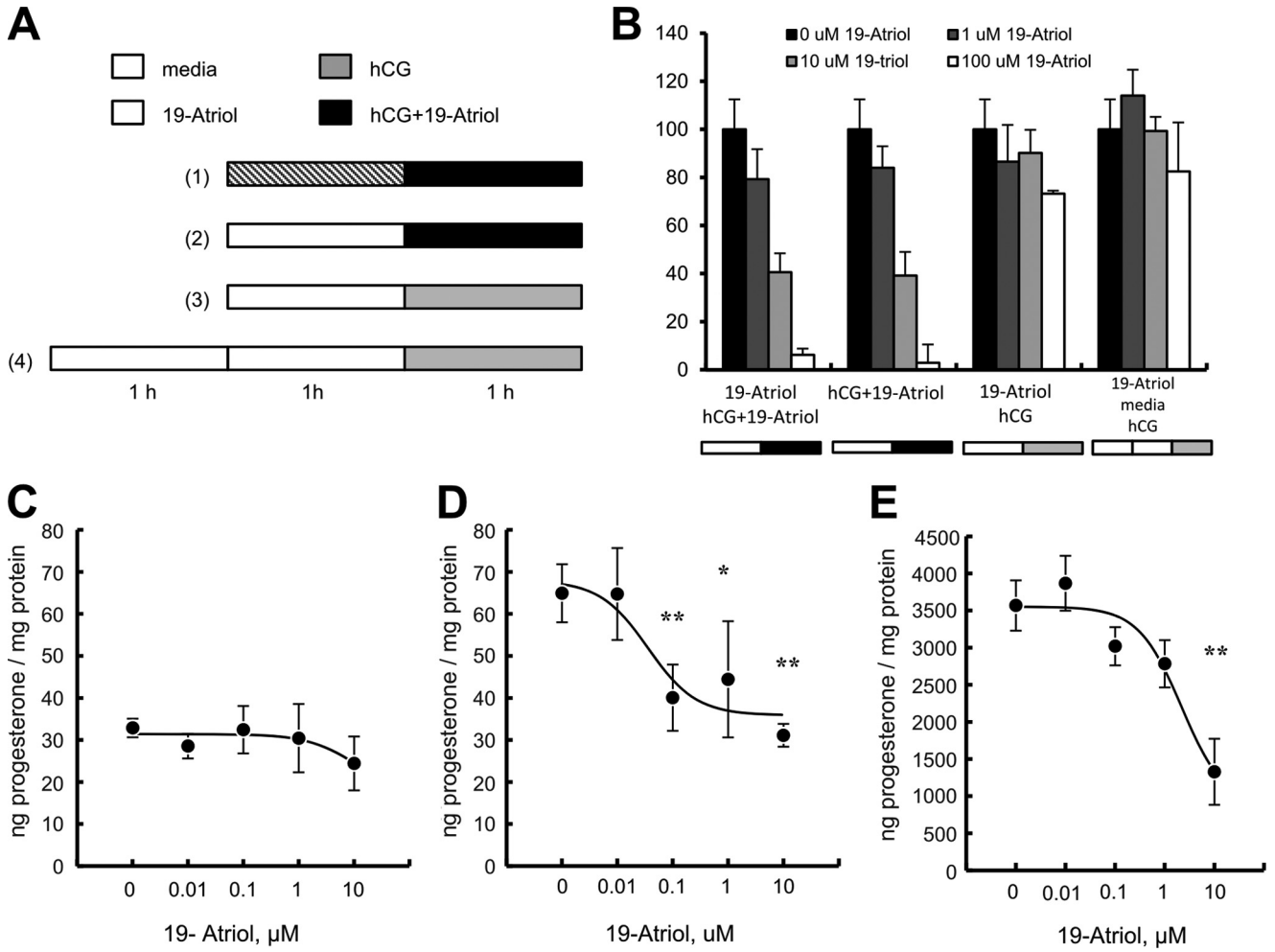

FIGURE 7. **19-Atriol wash-out effect on hormone-stimulated steroid biosynthesis and its impact on PK 11195-stimulated and constitutive steroidogenesis.** *A*, experimental design of wash-out showing the four treatments described under "Experimental Procedures." A 1-h incubation with either 0–100 μM 19-Atriol (*hatched bars*) or medium (*white bars*) was followed by wash-out and immediate stimulation with hCG + 0–100 μM 19-Atriol (*treatments 1* and *2*; *black bars*) or hCG (*treatment 3*; *gray bar*) for 1 h or incubation in medium for 1 h and then stimulation with hCG for 1 h (*treatment 4*). Steroid production after the 1-h treatment with hCG + 19-Atriol or hCG in the four treatments was then assessed by RIA. *B*, results of experiments described in *A*. The mean ± S.E. values (*error bars*) from three independent experiments are shown. The treatments are ordered as described in *A* and denoted with *bars* corresponding to the appropriate treatment. *C*, effect of 19-Atriol on basal steroidogenesis. MA-10 Leydig cells were incubated with increasing concentrations of 19-Atriol in the presence of medium, and steroid production was assessed by RIA. The mean ± S.E. values from three independent experiments are shown. *D*, effect of 19-Atriol on PK 11195-dependent steroidogenesis. MA-10 cells were incubated as in *A* but with 1 μM PK 11195 instead of medium. The mean ± S.E. values from three independent experiments are shown. **, $p < 0.01$; *, $p < 0.05$ by one-way ANOVA with Neumann-Keuls test. *E*, dose-dependent effect of 19-Atriol on constitutive steroidogenesis. R2C cells were cultured with increasing concentrations of 19-Atriol (0–10 μM) for 2 h in the medium, and progesterone production was assessed by RIA. Results are presented as the mean ± S.E. **, $p < 0.01$ by one-way ANOVA with Neumann-Keuls test.

bated with hCG + 19-Atriol (Fig. 7*B*, *column groups 1* and *2*). Interestingly, in keeping with the hypothesized solubility of 19-Atriol, wash-out of 19-Atriol almost immediately restored hCG-stimulated steroidogenesis at 1 and 10 μM 19-Atriol, with nearly complete restoration at 100 μM concentrations (Fig. 7*B*, *column group 3*). This reduction in hormone-stimulated steroidogenesis at 100 μM 19-Atriol was not due to overt toxicity, however, because an additional exposure to medium for 1 h after 19-Atriol exposure restored hCG-mediated steroidogenesis to control levels (Fig. 7*B*, *column group 4*). These data suggest that 19-Atriol acts as a chemical "on-off" switch for steroidogenesis, dissociating from the cells upon removal from medium and alleviating steroidogenic inhibition.

Steroidogenic cells synthesize steroids at low levels in the absence of hormonal stimulation. The finding that 19-Atriol restricts the total amount of steroid produced upon hormonal stimulation raised the question of its effect on basal steroidogenesis. MA-10 Leydig tumor cells were incubated in medium for 2 h in the presence of increasing concentrations of 19-Atriol that did not inhibit CYP11A1 (0–10 μM), and the progesterone synthesized was measured. As observed in Fig. 7*C*, 19-Atriol at the concentrations tested did not significantly affect basal progesterone synthesis by MA-10 cells, further supporting the hypothesis that the TSPO CRAC domain is instrumental in mediating high flux cholesterol movement.

In addition to hormonal exposure, steroidogenesis can be stimulated by TSPO ligands, such as PK 11195 (36). To examine whether 19-Atriol influences TSPO-mediated steroidogenesis in a manner similar to its effect on hormonally stimulated steroidogenesis, MA-10 cells were incubated with 1 μM PK 11195 in the presence of increasing concentrations of 19-Atriol (0–10 μM), and progesterone production was assessed by RIA. As

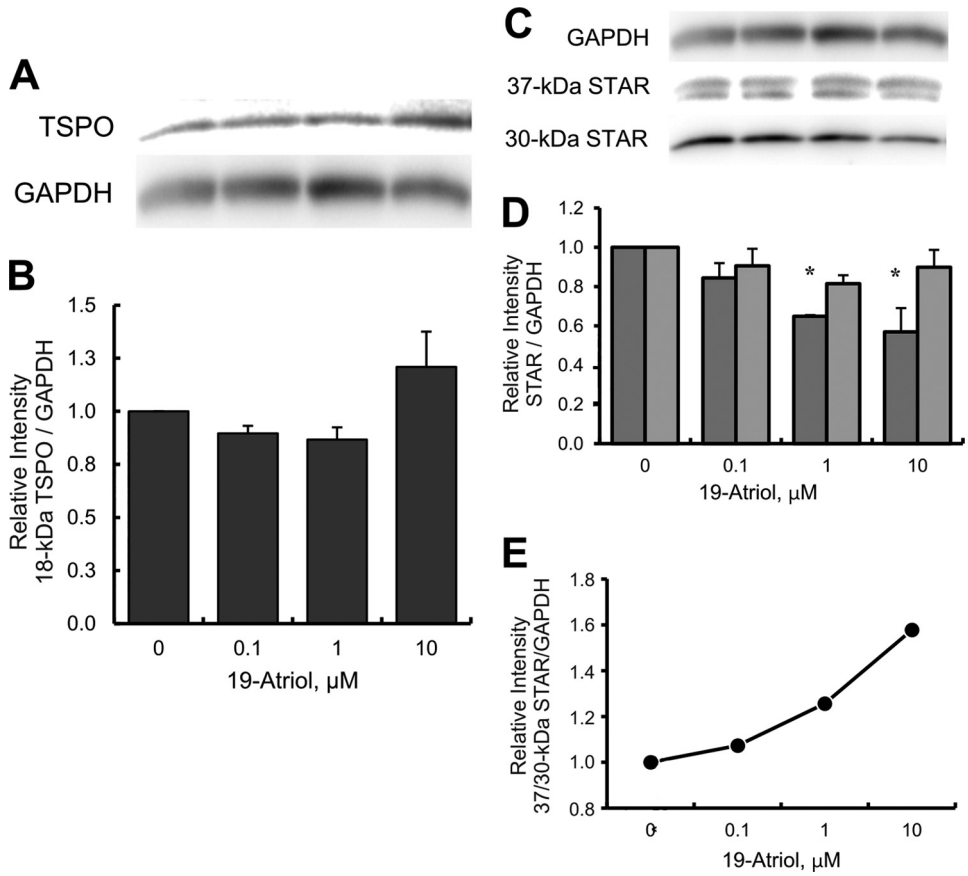

FIGURE 8. **Effect of 19-Atriol on TSPO and STAR protein expression.** *A*, a representative immunoblot is shown of 18-kDa TSPO and GAPDH levels in MA-10 Leydig cells treated with increasing concentrations of 19-Atriol (0–10 μM) in the presence of 1 mM dbcAMP for 2 h. Proteins were separated by SDS-PAGE and identified by immunoblot analysis, as described under "Experimental Procedures." *B*, quantification of 18-kDa TSPO protein levels normalized to GAPDH relative to control values from three independent experiments. *C*, a representative immunoblot is shown from MA-10 cells treated as described in *A*. Proteins were separated by SDS-PAGE, and immunoblotting was performed with an antibody that recognizes 30- and 37-kDa STAR isoforms. *D* and *E*, quantification of 30- and 37-kDa STAR protein levels (*D*), with 30-kDa STAR levels depicted in *dark gray* and 37-kDa STAR levels depicted in *light gray*, and ratio of 37- to 30-kDa STAR (*E*) from three independent experiments. *, $p < 0.05$ by one-way ANOVA.

shown in Fig. 7*D*, 19-Atriol inhibited PK 11195-mediated progesterone production in a dose-dependent manner, with an IC_{50} of 357 ± 332 nM. Importantly, 19-Atriol returned progesterone production in the PK 11195 cells to basal levels (Fig. 7, compare *A* and *B*). These results demonstrate the specificity of 19-Atriol for TSPO-mediated steroid production and suggest that the CRAC domain is instrumental for high flux mitochondrial cholesterol movement elicited by hormonal or drug stimulation.

Steroid biosynthesis is both initiated and sustained by continual hormonal stimulation (48). The MA-10 mouse tumor cell line is an excellent model for the study of steroidogenic initiation, whereas the constitutively steroidogenic R2C rat tumor cell line serves to model sustained steroid biosynthesis. TSPO has previously been shown to be essential for this constitutive steroid biosynthesis in the R2C line (55). To assess the ability of 19-Atriol to control sustained steroidogenesis, R2C cells were cultured in the presence of increasing concentrations (0–10 μM) of 19-Atriol for 2 h, and progesterone released into the medium was measured by RIA (Fig. 7*E*). A similar dose response was observed in R2C as had been observed in MA-10 cells with an IC_{50} of 3.58 ± 1.56 μM. Thus, 19-Atriol can limit the initiation and sustainment of steroidogenic flux in Leydig cells from multiple species.

CRAC Domain Inhibition and Mitochondrial Protein Processing—Decreases in TSPO protein levels are linked to decreased steroidogenic capacity, as evidenced by antisense oligonucleotide and disruptive homologous recombination experiments (38, 55). To assess whether the decreased steroidogenic capacity of the MA-10 cells exposed to 19-Atriol was a consequence of increased turnover of the TSPO protein, we exposed MA-10 cultures to dbcAMP and increasing concentrations of 19-Atriol (0–10 μM) for 2 h. Protein immunoblotting revealed no significant changes in 18-kDa TSPO protein levels at any of the concentrations tested (Fig. 8, *A* and *B*), indicating that 19-Atriol does not affect expression or turnover of the TSPO protein. Although not significant, a trend existed toward increased levels of 18-kDa TSPO protein at the highest concentrations of 19-Atriol used.

Previous studies have demonstrated that inhibition of TSPO expression by antisense oligodeoxynucleotides or TSPO function using a peptide targeted against the drug binding domain inhibits STAR protein import into the mitochondria, as evidenced by decreased levels of 30-kDa STAR protein and increased 37-kDa STAR protein levels (38). To examine the effect of CRAC domain inhibition on STAR protein import and processing, MA-10 cell cultures were incubated with dbcAMP and increasing concentrations of 19-Atriol (0–10 μM) for 2 h,

after which the levels of 30- and 37-kDa STAR proteins were assessed by SDS-PAGE followed by immunoblot analysis. A representative immunoblot is shown in Fig. 8*C*, and quantification of multiple experiments is demonstrated in Fig. 8*D*. As can be observed, 19-Atriol significantly decreased the 30-kDa STAR protein levels while exhibiting little effect on the 37-kDa preprotein. Plotting the ratio of 37-kDa *versus* 30-kDa STAR proteins in Fig. 8*E* demonstrates a clear difference between the two protein populations, suggesting that STAR import and/or processing is inhibited by the CRAC domain ligand 19-Atriol.

DISCUSSION

Cholesterol serves as the precursor of all steroids. In vertebrates, the first step in the steroidogenic process is the metabolism of cholesterol to pregnenolone in the mitochondrial matrix by the cytochrome P450 enzyme CYP11A1 (4). To reach the mitochondrial matrix, cholesterol must traverse the outer and inner mitochondrial membranes, a process that is induced by hormonal stimulation in steroidogenic tissues (3). Hormonal stimulation, which principally operates through a cAMP-mediated signaling pathway (1, 2), targets a multiprotein complex, named the transduceosome (6), at the outer mitochondrial membrane. The transduceosome is composed of both cytoplasmic components, such as the prominently described hormone-induced STAR protein (8), and integral mitochondrial membrane proteins, such as the TSPO protein (18). TSPO is highly expressed in steroidogenic tissues (18, 23), and silencing of its expression potently inhibits the steroidogenic capacity of Leydig tumor cells, even in the presence of the STAR protein (38). These findings strongly implicated TSPO in mitochondrial cholesterol transport in steroidogenesis.

The role for TSPO in mitochondrial cholesterol transfer was further supported by the discovery of a high affinity cholesterol binding site, termed the CRAC domain, located at the proximal C terminus of the polypeptide chain (25). This CRAC motif, defined by the algorithm (L/V)X_{1-5}YX_{1-5}(R/K), was further described in several other proteins that associate with cholesterol, including CYP11A1 (25), caveolin (29), acetylcholine esterase (31), and the gp41 peptide of the HIV-1 virus (30). Moreover, this motif is very often associated with the functionality of the protein in question. For example, mutation of the CRAC motif in gp41 results in reduced virulence (30), and deletion of the TSPO CRAC motif ablates the ability of the protein to mediate cholesterol uptake when expressed in *E. coli* (25). NMR spectroscopy of the TSPO CRAC motif demonstrated that the side chains of the motif generated a groove capable of accommodating a cholesterol molecule, with the central tyrosine playing a critical role in cholesterol binding (28). Collectively, these findings suggested that the CRAC domain is critical for TSPO function regarding cholesterol transport, although molecular details remain to be elucidated.

To help establish a useful tool to investigate the molecular mechanisms of the TSPO CRAC motif, we undertook molecular modeling studies to identify novel ligands for the CRAC domain. To this end, we generated homology models of the CRAC domains of several species and used them to screen commercially available chemical libraries. Energy minimization of the structure in the presence of cholesterol produced a structure hypothesized to be active in mitochondrial cholesterol transport. In addition, these computational modeling studies of the TSPO CRAC domain independently corroborated previously performed NMR studies on the structure of the CRAC peptide in solution (28), with the central tyrosine and C-terminal arginine forming hydrogen bonds with the cholesterol molecule in a groove formed by the CRAC motif residues (Fig. 1*B*). Interestingly, the central tyrosine and C-terminal lysine of the HIV-1 gp41 CRAC motif, corresponding to the Tyr and Arg of the TSPO CRAC, were computationally modeled to form hydrogen bonds with cholesterol (56, 57), suggesting common molecular interactions in these motifs.

In silico screening of commercially available chemical libraries yielded 19 "best" hypothetical hits, based on predicted binding energy and docking scores (a metric of spatial fit). Bioactivity screening of the ability of these CRAC ligands to significantly inhibit cAMP-mediated steroidogenesis demonstrated that only steroid adducts and substituted steroid families produced significant hits (Fig. 3, *A* and *B*), although these compounds fell in the weaker predicted binding group. However, notably, the best active steroidal structures (19-Atriol and 5957219) were found with high binding energy and docking scores within the steroidal binding set, and similarly, the average active non-steroidal structures (5754198 and 6524457) have higher binding energy and dock scores compared with low active structures within the non-steroidal set (Fig. 2*A*). These studies prompted us to conclude that although the binding capacity is only one variable contributing to CRAC-ligand associations (as evidenced by compounds with similar binding scores but no bioactivity), a slightly weaker interaction appears optimal for CRAC motif interactions. This hypothesis is supported by a study with the gp41 HIV-1 CRAC motif, which demonstrated that the most biologically active CRAC sequence weakly interacted with the cholesterol ring structures, whereas less biologically active sequences form extensive contacts with the hydrocarbon rings of the sterol backbone (56).

The CRAC ligand most efficacious in suppressing steroidogenesis was the substituted steroid, 19-Atriol (3,17,19-androsten-5-triol). Like cholesterol, 19-Atriol could displace binding of cross-linkable promegestone to an isolated CRAC domain peptide, a qualitative assay of CRAC domain binding (27). 19-Atriol was not as effective as cholesterol, with an IC_{50} higher than that of cholesterol. Further examination of the dose dependence of 19-Atriol inhibition of [^{3}H]promegestone cross-linking to that CRAC motif *in vitro* and *in situ* in hormone-mediated steroidogenesis in MA-10 mouse Leydig tumor cells revealed a good correlation between the two parameters, with significant inhibition of promegestone binding and steroidogenesis occurring in the low (1–10 μM) range. Similar results were observed in the constitutively steroidogenic R2C rat Leydig tumor cell line, demonstrating that 19-Atriol controls both the initiation and sustainment of steroidogenesis in multiple species and inhibiting hormone-induced or constitutive high flux cholesterol transfer. Moreover, this inhibition was dependent upon the constant presence of 19-Atriol because wash-out studies demonstrated that 19-Atriol removal nearly immediately restores hormone-mediated steroidogenesis and suggested that 19-Atriol does not remain bound to TSPO. Further

experiments with radiolabeled 19-Atriol will be required to confirm this hypothesis.

Studies with 22*R*-HC, a water-soluble cholesterol analog that bypasses the mitochondrial cholesterol transfer step and is directly metabolized to pregnenolone by CYP11A1, confirmed that 19-Atriol operated at the level of mitochondrial cholesterol transfer because steroid production with this stimulant was unaffected within the 1–10 μM range. Interestingly, at higher 19-Atriol concentrations, steroidogenesis in the presence of 22*R*-HC was significantly reduced. These results suggest that CYP11A1 is inhibited by 19-Atriol at higher concentrations. This is interesting because CYP11A1 possesses a putative CRAC domain in its catalytic site (25, 54), suggesting that the variations in CRAC motif sequences observed in different proteins may offer conformational stereoselectivity for the binding of different ligands.

There was no evident cellular or mitochondrial toxicity at the concentrations of 19-Atriol used (0–100 μM) in either MA-10 Leydig or MDA-MB-231 breast cancer tumor cells (Fig. 5, *A–C*, and supplemental Fig. 1), both of which are rich in TSPO (58). This was further supported by the finding that upon removal of 19-Atriol, even at 100 μM, MA-10 cells regained their ability to form steroids in response to hCG.

Although blockage of cholesterol binding to the TSPO CRAC domain by 19-Atriol appears sufficient to block hormonally induced mitochondrial cholesterol transfer, additional events may be affected by 19-Atriol exposure. Oxysterols have been shown to associate with the endoplasmic reticulum anchor Insig proteins, inhibiting cholesterol biosynthesis by helping to retain the SREBP transcription factor in the endoplasmic reticulum (59). Overnight exposure of MA-10 cells to 19-Atriol did not affect total cholesterol levels in these cells, suggesting that 19-Atriol does not affect components of the cholesterol biosynthesis pathway (supplemental Fig. 2). Other cholesterol-interacting proteins more directly associated with steroidogenesis may be affected by 19-Atriol, however. STAR and its STAR-related lipid transfer (START) domain (60) have been demonstrated to bind fluorescent cholesterol analogs (61), and mutations in the START domain disrupt binding of these analogs and, in correlation, impair STAR-mediated steroidogenesis. Such mutations were identified as being responsible for the lethal human pathology of congenital adrenal hyperplasia (62). The START domain pocket for cholesterol is quite large compared with the sterol (63), and our molecular modeling of the START domain has indicated that this pocket may accommodate the smaller 19-Atriol model.[4] Although definitive tests of the possible 19-Atriol interaction with STAR are currently under way, we did investigate its effect on STAR import and processing. Previous work has demonstrated that suppression of TSPO expression and inhibition of the drug binding site with a targeting peptide inhibits the import and processing of the 37-kDa STAR precursor to the 30-kDa mitochondrial STAR protein (38). Exposure of cells to 19-Atriol elicited a similar effect, leaving the 37-kDa STAR protein intact while inhibiting formation of the 30-kDa processing product (Fig. 8, *C–E*). Because mutational perturbation of the START domain of STAR (which would be affected by 19-Atriol) does not inhibit mitochondrial import (64), these findings support a model of direct effect of 19-Atriol on TSPO. Furthermore, these findings lend further support to our previous demonstration of the requirement of TSPO for mitochondrial import and/or processing of STAR (37, 38).

Further specificity of the 19-Atriol interaction with TSPO is derived from studies with the drug PK 11195, which binds the drug-binding site of TSPO (22) and stimulates steroidogenesis (36). 19-Atriol inhibited PK 11195-induced steroid synthesis at concentrations an order of magnitude lower than those required to inhibit hCG- or dbcAMP-stimulated steroidogenesis (Fig. 6*A versus* Fig. 7*B*). This result is not surprising because hormonal stimulation initiates a diversity of cellular processes (6), whereas PK 11195 binds and stimulates TSPO. Taken together, these results further support the specificity of action of 19-Atriol against TSPO. Interestingly, 19-Atriol had no effect on PK 11195 binding to mitochondrial preparations at concentrations that inhibited steroidogenesis (Fig. 4*A*). This is an important finding because it argues that the drug-binding site of TSPO and the natural ligand DBI operate upstream of the CRAC domain in the mechanism of action of TSPO. This observation will be useful in further understanding the molecular mechanisms involved in mitochondrial cholesterol transport.

In conclusion, we have successfully identified a ligand for the CRAC motif of TSPO that can control steroidogenesis. This compound could serve as a useful tool for studying the function of TSPO in cholesterol transport. It may also serve as a useful lead compound for the design of drugs used in the treatment of conditions of excessive steroid production, including Cushing's syndrome, a condition of hypercortisolism with elevated morbidity and mortality (65), and cases of gonadal and adrenal steroid-producing tumors (66, 67). Pharmacological treatments meant to normalize pathological steroidogenesis are currently being developed, and one can fairly propose that 19-Atriol and potential derivatives may well suit this new therapeutic strategy. In addition, 19-Atriol and its derivatives could also be used to normalize altered neurosteroid synthesis in the brain that can be linked to various pathologies (68, 69). Investigations of the effects of 19-Atriol in various organisms will also give further insight into the physiological function of TSPO because it will provide an acute modifier of TSPO function *in vivo*, which is useful for its experimentally diminishing function after the embryonically lethal developmental window observed in *Tspo* knock-out mice (70).

Acknowledgments—We kindly thank Dr. Mario Ascoli (University of Iowa, Iowa City, IA) for supplying the MA-10 cell line, Dr. Buck Hales (University of Southern Illinois, Carbondale, IL) for the STAR antiserum, and the National Hormone and Pituitary Program (NICHD, National Institutes of Health) for supplying the hCG.

[4] N. Akula, A. Midzak, L. Lecanu, and V. Papadopoulos, unpublished data.

REFERENCES

1. Ascoli, M., Fanelli, F., and Segaloff, D. L. (2002) *Endocr. Rev.* **23,** 141–174
2. Spät, A., and Hunyady, L. (2004) *Physiol. Rev.* **84,** 489–539
3. Jefcoate, C. (2002) *J. Clin. Invest.* **110,** 881–890

4. Payne, A. H., and Hales, D. B. (2004) *Endocr. Rev.* **25,** 947–970
5. Papadopoulos, V., Liu, J., and Culty, M. (2007) *Mol. Cell. Endocrinol.* **265,** 59–64
6. Rone, M. B., Fan, J., and Papadopoulos, V. (2009) *Biochim. Biophys. Acta* **1791,** 646–658
7. Christenson, L. K., and Strauss, J. F., 3rd (2000) *Biochim. Biophys. Acta* **1529,** 175–187
8. Miller, W. L. (2007) *Biochim. Biophys. Acta* **1771,** 663–676
9. King, S. R., Ronen-Fuhrmann, T., Timberg, R., Clark, B. J., Orly, J., and Stocco, D. M. (1995) *Endocrinology* **136,** 5165–5176
10. Pon, L. A., and Orme-Johnson, N. R. (1986) *J. Biol. Chem.* **261,** 6594–6599
11. Stocco, D. M., and Kilgore, M. W. (1988) *Biochem. J.* **249,** 95–103
12. Clark, B. J., Wells, J., King, S. R., and Stocco, D. M. (1994) *J. Biol. Chem.* **269,** 28314–28322
13. Bose, H. S., Lingappa, V. R., and Miller, W. L. (2002) *Nature* **417,** 87–91
14. Bose, M., Whittal, R. M., Miller, W. L., and Bose, H. S. (2008) *J. Biol. Chem.* **283,** 8837–8845
15. Arakane, F., King, S. R., Du, Y., Kallen, C. B., Walsh, L. P., Watari, H., Stocco, D. M., and Strauss, J. F., 3rd (1997) *J. Biol. Chem.* **272,** 32656–32662
16. Clark, B. J., Ranganathan, V., and Combs, R. (2001) *Mol. Cell. Endocrinol.* **173,** 183–192
17. Li, H., Degenhardt, B., Tobin, D., Yao, Z. X., Tasken, K., and Papadopoulos, V. (2001) *Mol. Endocrinol.* **15,** 2211–2228
18. Papadopoulos, V., Baraldi, M., Guilarte, T. R., Knudsen, T. B., Lacapère, J. J., Lindemann, P., Norenberg, M. D., Nutt, D., Weizman, A., Zhang, M. R., and Gavish, M. (2006) *Trends Pharmacol. Sci.* **27,** 402–409
19. Braestrup, C., and Squires, R. F. (1977) *Proc. Natl. Acad. Sci. U.S.A.* **74,** 3805–3809
20. Garnier, M., Dimchev, A. B., Boujrad, N., Price, J. M., Musto, N. A., and Papadopoulos, V. (1994) *Mol. Pharmacol.* **45,** 201–211
21. Gavish, M., Bachman, I., Shoukrun, R., Katz, Y., Veenman, L., Weisinger, G., and Weizman, A. (1999) *Pharmacol. Rev.* **51,** 629–650
22. Le Fur, G., Perrier, M. L., Vaucher, N., Imbault, F., Flamier, A., Benavides, J., Uzan, A., Renault, C., Dubroeucq, M. C., and Guérémy, C. (1983) *Life Sci.* **32,** 1839–1847
23. Papadopoulos, V. (1993) *Endocr. Rev.* **14,** 222–240
24. Wendler, G., Lindemann, P., Lacapère, J. J., and Papadopoulos, V. (2003) *Biochem. Biophys. Res. Commun.* **311,** 847–852
25. Li, H., and Papadopoulos, V. (1998) *Endocrinology* **139,** 4991–4997
26. Lacapère, J. J., Delavoie, F., Li, H., Péranzi, G., Maccario, J., Papadopoulos, V., and Vidic, B. (2001) *Biochem. Biophys. Res. Commun.* **284,** 536–541
27. Li, H., Yao, Z., Degenhardt, B., Teper, G., and Papadopoulos, V. (2001) *Proc. Natl. Acad. Sci. U.S.A.* **98,** 1267–1272
28. Jamin, N., Neumann, J. M., Ostuni, M. A., Vu, T. K., Yao, Z. X., Murail, S., Robert, J. C., Giatzakis, C., Papadopoulos, V., and Lacapère, J. J. (2005) *Mol. Endocrinol.* **19,** 588–594
29. Epand, R. F., Sayer, B. G., and Epand, R. M. (2005) *Biochemistry* **44,** 5525–5531
30. Epand, R. M., Sayer, B. G., and Epand, R. F. (2005) *J. Mol. Biol.* **345,** 339–350
31. Xie, H. Q., Liang, D., Leung, K. W., Chen, V. P., Zhu, K. Y., Chan, W. K., Choi, R. C., Massoulié, J., and Tsim, K. W. (2010) *J. Biol. Chem.* **285,** 11537–11546
32. Joseph-Liauzun, E., Farges, R., Delmas, P., Ferrara, P., and Loison, G. (1997) *J. Biol. Chem.* **272,** 28102–28106
33. Culty, M., Li, H., Boujrad, N., Amri, H., Vidic, B., Bernassau, J. M., Reversat, J. L., and Papadopoulos, V. (1999) *J. Steroid Biochem. Mol Biol.* **69,** 123–130
34. Korkhov, V. M., Sachse, C., Short, J. M., and Tate, C. G. (2010) *Structure* **18,** 677–687
35. Krueger, K. E., and Papadopoulos, V. (1990) *J. Biol. Chem.* **265,** 15015–15022
36. Papadopoulos, V., Mukhin, A. G., Costa, E., and Krueger, K. E. (1990) *J. Biol. Chem.* **265,** 3772–3779
37. Gazouli, M., Han, Z., and Papadopoulos, V. (2002) *J. Pharmacol. Exp. Ther.* **303,** 627–632
38. Hauet, T., Yao, Z. X., Bose, H. S., Wall, C. T., Han, Z., Li, W., Hales, D. B., Miller, W. L., Culty, M., and Papadopoulos, V. (2005) *Mol. Endocrinol.* **19,** 540–554
39. Shin, S. I., Yasumura, Y., and Sato, G. H. (1968) *Endocrinology* **82,** 614–616
40. Sali, A., Potterton, L., Yuan, F., van Vlijmen, H., and Karplus, M. (1995) *Proteins* **23,** 318–326
41. Altschul, S. F., Madden, T. L., Schäffer, A. A., Zhang, J., Zhang, Z., Miller, W., and Lipman, D. J. (1997) *Nucleic Acids Res.* **25,** 3389–3402
42. Vassylyev, D. G., Tomitori, H., Kashiwagi, K., Morikawa, K., and Igarashi, K. (1998) *J. Biol. Chem.* **273,** 17604–17609
43. Boulanger, M. J., Chow, D. C., Brevnova, E. E., and Garcia, K. C. (2003) *Science* **300,** 2101–2104
44. Martin, Y. C. (1992) *J. Med. Chem.* **35,** 2145–2154
45. Kramer, B., Rarey, M., and Lengauer, T. (1999) *Proteins* **37,** 228–241
46. Mosmann, T. (1983) *J. Immunol. Methods* **65,** 55–63
47. Bradford, M. M. (1976) *Anal. Biochem.* **72,** 248–254
48. Artemenko, I. P., Zhao, D., Hales, D. B., Hales, K. H., and Jefcoate, C. R. (2001) *J. Biol. Chem.* **276,** 46583–46596
49. Kuntz, I. D. (1992) *Science* **257,** 1078–1082
50. Goodsell, D. S., and Olson, A. J. (1990) *Proteins* **8,** 195–202
51. Clark, R. D., Strizhev, A., Leonard, J. M., Blake, J. F., and Matthew, J. B. (2002) *J. Mol. Graph. Model.* **20,** 281–295
52. Veenman, L., Shandalov, Y., and Gavish, M. (2008) *J. Bioenerg. Biomembr.* **40,** 199–205
53. Allen, J. A., Shankara, T., Janus, P., Buck, S., Diemer, T., Hales, K. H., and Hales, D. B. (2006) *Endocrinology* **147,** 3924–3935
54. Pikuleva, I. A., Mackman, R. L., Kagawa, N., Waterman, M. R., and Ortiz de Montellano, P. R. (1995) *Arch. Biochem. Biophys.* **322,** 189–197
55. Papadopoulos, V., Amri, H., Li, H., Boujrad, N., Vidic, B., and Garnier, M. (1997) *J. Biol. Chem.* **272,** 32129–32135
56. Epand, R. F., Thomas, A., Brasseur, R., Vishwanathan, S. A., Hunter, E., Epand, R. M. (2006) *Biochemistry* **45,** 6105–6114
57. Vishwanathan, S. A., Thomas, A., Brasseur, R., Epand, R. F., Hunter, E., and Epand, R. M. (2008) *Biochemistry* **47,** 124–130
58. Hardwick, M., Fertikh, D., Culty, M., Li, H., Vidic, B., and Papadopoulos, V. (1999) *Cancer Res.* **59,** 831–842
59. Radhakrishnan, A., Ikeda, Y., Kwon, H. J., Brown, M. S., and Goldstein, J. L. (2007) *Proc. Natl. Acad. Sci. U.S.A.* **104,** 6511–6518
60. Alpy, F., and Tomasetto, C. (2005) *J. Cell Sci.* **118,** 2791–2801
61. Petrescu, A. D., Gallegos, A. M., Okamura, Y., Strauss, J. F., 3rd, and Schroeder, F. (2001) *J. Biol. Chem.* **276,** 36970–36982
62. Lin, D., Sugawara, T., Strauss, J. F., 3rd, Clark, B. J., Stocco, D. M., Saenger, P., Rogol, A., and Miller, W. L. (1995) *Science* **267,** 1828–1831
63. Tsujishita, Y., and Hurley, J. H. (2000) *Nat. Struct. Biol.* **7,** 408–414
64. Granot, Z., Geiss-Friedlander, R., Melamed-Book, N., Eimerl, S., Timberg, R., Weiss, A. M., Hales, K. H., Hales, D. B., Stocco, D. M., and Orly, J. (2003) *Mol. Endocrinol.* **17,** 2461–2476
65. Shalet, S., and Mukherjee, A. (2008) *Curr. Opin. Endocrinol. Diabetes Obes.* **15,** 234–238
66. Freeman, D. A. (1986) *Endocr. Rev.* **7,** 204–220
67. Bornstein, S. R., Stratakis, C. A., and Chrousos, G. P. (1999) *Ann. Int. Med.* **130,** 759–771
68. Follesa, P., Biggio, F., Talani, G., Murru, L., Serra, M., Sanna, E., and Biggio, G. (2006) *Psychopharmacology* **186,** 267–280
69. Gomez-Sanchez, E. P., Gomez-Sanchez, C. M., Plonczynski, M., and Gomez-Sanchez, C. E. (2010) *Exp. Physiol.* **95,** 120–130
70. Lacapère, J. J., and Papadopoulos, V. (2003) *Steroids* **68,** 569–585